Experimental demonstration of adaptive digital monitoring and compensation of chromatic dispersion for coherent DP-QPSK receiver

Borkowski, Robert; Zhang, Xu; Zibar, Darko; Younce, Richard; Tafur Monroy, Idelfonso

Published in:
Optics Express

Link to article, DOI:
10.1364/OE.19.00B728

Publication date:
2011

Document Version
Publisher's PDF, also known as Version of record

Experimental demonstration of adaptive digital monitoring and compensation of chromatic dispersion for coherent DP-QPSK receiver

Robert Borkowski,[1,*] **Xu Zhang,**[1] **Darko Zibar,**[1] **Richard Younce,**[2] **and Idelfonso Tafur Monroy**[1]

[1] *DTU Fotonik, Department of Photonics Engineering, Technical University of Denmark, Ørsteds Plads, Building 343, DK-2800 Kgs. Lyngby, Denmark*
[2] *Tellabs, 1415 West Diehl Road, Naperville, IL 60563, USA*
[*] *rbor@fotonik.dtu.dk*

Abstract: We experimentally demonstrate a digital signal processing (DSP)-based optical performance monitoring (OPM) algorithm for in-service monitoring of chromatic dispersion (CD) in coherent transport networks. Dispersion accumulated in 40 Gbit/s QPSK signal after 80 km of fiber transmission is successfully monitored and automatically compensated without prior knowledge of fiber dispersion coefficient. Four different metrics for assessing CD mitigation are implemented and simultaneously verified proving to have high estimation accuracy. No observable penalty is measured when the monitoring module drives an adaptive digital CD equalizer.

OCIS codes: (060.1660) Coherent communications; (060.2330) Fiber optics communications.

References and links

1. S. J. Savory, "Digital filters for coherent optical receivers," Opt. Express **16**, 804–817 (2008).
2. F. Hauske, J. Geyer, M. Kuschnerov, K. Piyawanno, T. Duthel, C. Fludger, D. van den Borne, E. Schmidt, B. Spinnler, H. de Waardt, and B. Lankl, "Optical performance monitoring from FIR filter coefficients in coherent receivers," in *Optical Fiber Communication Conference*, OSA Technical Digest (CD) (Optical Society of America, 2008), paper OThW2.
3. M. Kuschnerov, F. N. Hauske, K. Piyawanno, B. Spinnler, A. Napoli, and B. Lankl, "Adaptive chromatic dispersion equalization for non-dispersion managed coherent systems," in *Optical Fiber Communication Conference*, OSA Technical Digest (CD) (Optical Society of America, 2009), paper OMT1.
4. F. N. Hauske, C. Xie, Z. P. Zhang, C. Li, L. Li, and Q. Xiong, "Frequency domain chromatic dispersion estimation," in *Optical Fiber Communication Conference*, OSA Technical Digest (CD) (Optical Society of America, 2010), paper JThA11.
5. D. Wang, C. Lu, A.P.T Lau, and S. He, "Adaptive chromatic dispersion compensation for coherent communication systems using delay-tap sampling technique," IEEE Photon. Technol. Lett. **14**, 1016–1018 (2011).
6. B. Spinnler, "Equalizer design and complexity for digital coherent receivers," IEEE J. Sel. Topics Quantum Electron. **5**, 1180–1192 (2010).
7. M. Kuschnerov, F. N. Hauske, K. Piyawanno, B. Spinnler, M.S. Alfiad, A. Napoli, and B. Lankl, "DSP for coherent single-carrier receivers," J. Lightwave Technol. **27**, 3614–3622 (2009).
8. S. Haykin, *Adaptive filter theory* (Prentice-Hall, 2002).

#155788 - $15.00 USD Received 3 Oct 2011; revised 25 Nov 2011; accepted 26 Nov 2011; published 6 Dec 2011

1. Introduction

Coherent optical communication is already a commercially well established technology. One of the advantages of coherent receivers is that DSP algorithms, specifically impairment equalization schemes, can be implemented directly in the receivers' electronics. Chromatic dispersion, one of the most important factors contributing to signal degradation in long and ultra long haul optical communication systems, can be relatively easy canceled in the DSP circuit of a coherent receiver [1]. This enables operation of dispersion non-compensated links due to the fact that dispersion maps or CD compensation units are no longer necessary to ensure best reception quality and minimize number of received bit errors. Nonetheless, even for DSP-based dispersion filters it is usually assumed that CD value that accumulates in the signal is both known and constant enabling the use of a static CD filter at the receiver. Although this assumption is valid in submarine or terrestrial point-to-point links, it does not hold when mixed or coherent transport networks with routing capabilities are considered. In the general case, CD value of the incoming signal may change dynamically. This challenge is addressed by a DSP-based CD monitoring subsystem.

In literature different approaches to CD monitoring directly from the received data (blind monitoring) have been presented, such as: parameter extraction from FIR filter coefficients [2], time- [3] or frequency-domain [4] monitors placed before timing recovery stage and delay-tap sampling technique [5].

On the other hand, as to the authors' knowledge, no experimental trial of a monitoring module preceding timing recovery has been performed so far. In this paper we report on a successful experimental demonstration of CD estimation using the aforementioned method. We show that the receiver can adaptively adjust in order to mitigate signal degradation due to CD, even without prior knowledge of the fiber dispersion coefficient.

2. Blind chromatic dispersion monitoring for digital coherent receivers

We consider a polarization-division-multiplexing (PDM) quadrature phase-shift keying (QPSK) receiver consisting of the optical front-end and a DSP part, as shown in Fig. 1. The incoming optical signal is photodetected and sampled by analog-to-digital converters (ADCs) operating at twice the symbol rate. The CD monitor and equalizer block, which is of interest

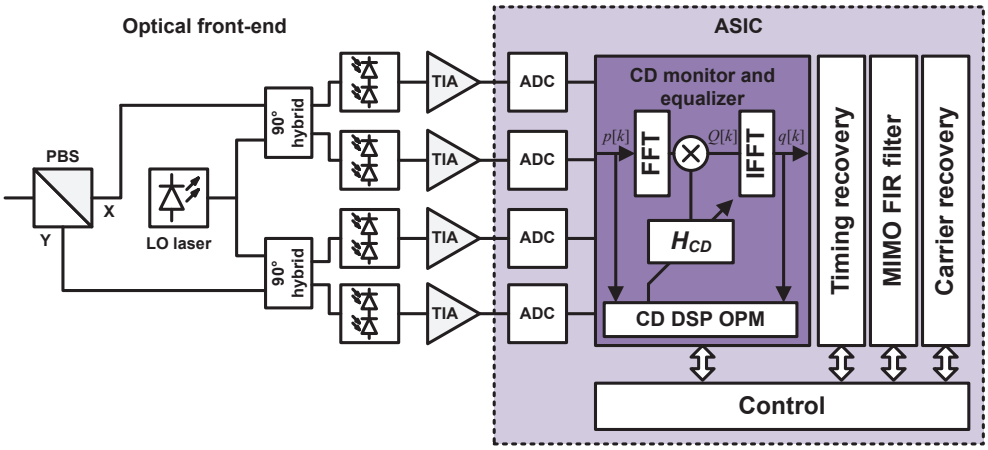

Fig. 1. Typical structure of a digital coherent receiver with CD monitoring and equalization block. The receiver in the figure monitors CD from time domain samples.

#155788 - $15.00 USD Received 3 Oct 2011; revised 25 Nov 2011; accepted 26 Nov 2011; published 6 Dec 2011

to this paper, is used for estimating and performing adaptive equalization of chromatic dispersion. Next, timing recovery takes place. A short, 7-tap finite impulse response (FIR) filter is then used for polarization demultiplexing and mitigation of residual impairments. Finally, carrier recovery is performed.

2.1. Generic scanning algorithm

The CD monitor and equalizer block in Fig. 1 uses a variable, transversal, frequency domain equalizer (FDE) for cancelation of inter-symbol interference (ISI) due to CD. The incoming signal $p[k]$ representing received complex optical field is first divided into blocks of length N, indexed consecutively with $k = 0 \ldots N-1$, and transformed to frequency domain. The resulting signal is then multiplied with the H_{CD} digital filter

$$H_{CD} = \exp\left(j f^2 \pi \frac{\lambda^2}{c} CD \right), \tag{1}$$

where f is the clock frequency, λ the signal wavelength, c the speed of light and CD the value of CD. The rationale behind using an FDE is the number of required complex multiplications as compared to time domain approach [6]. Next, the signal $Q[k]$ obtained after multiplication is transformed back to time domain as $q[k]$ and constitutes the output of the equalizer. Signals p and q (or Q, depending on particular method) are fed to a CD DSP OPM module which computes the metric J. Since the value of CD present in the channel is unknown, the transfer function H_{CD} may not be computed. However, due to the fact that H_{CD} has only one degree of freedom, adaptation can be performed by sweeping over a range of CD parameter, every time updating H_{CD}, until an optimal operating point is found. An interest range of CD values shall be specified, which in general will be different for each optical network and may depend on the topology and traffic characteristic. The CD parameter can be initialized as to coincide with the most probable CD value of the received signal in order to increase the convergence speed. The space of CD parameter is then gradually searched with a given resolution and the metric $J[CD]$ is computed for every value of CD under test.

As an engineering rule, CD scanning resolution for a simple maximum or minimum search-based metric shall not exceed 300 ps/nm with a recommended value of 200 ps/nm for a 28 Gbaud signal, which scales proportionally to the symbol rate squared. Once metric has been computed for all values lying within the range of interest, the metric is examined for a particular feature (e.g. minimum or maximum) which indicates the value of CD parameter that should be used to recalculate H_{CD} to mitigate the CD ISI.

The algorithm can be further extended to take average of the metric over multiple blocks or include multiple passes, each time narrowing the scanning range and increasing the scanning resolution. An example of a two-pass scan based on experimental data is shown in Fig. 2. Range between 0 ps/nm and 4000 ps/nm is swept with a step of 200 ps/nm (coarse scan). Once this initial estimate is obtained, a second pass with a resolution of only 20 ps/nm sets in and ranges 800 ps/nm centered around the previously found estimate (fine scan). This allows to increase the accuracy of the estimation. In theory, if no other impairment than CD is present in the signal, the maximum estimation error should be half of the scanning resolution. In practice, estimation error resulting from a single run is much greater because metrics are computed from blocks of finite length. Nonetheless, the accuracy of CD estimation at this stage is not strictly important because residual CD is compensated in the MIMO FIR filter that follows the CD equalizer in the receiver's DSP chain (comp. Fig. 1).

#155788 - $15.00 USD Received 3 Oct 2011; revised 25 Nov 2011; accepted 26 Nov 2011; published 6 Dec 2011

2.2. *Dispersion metrics*

This section provides a brief overview of algorithms for metrics computation. Four different metrics were implemented and experimentally verified in a transmission experiment. Figure 2 shows a comparison of those metrics generated from an experimental transmission of 20 Gbaud QPSK signal in a channel with 1280 ps/nm CD.

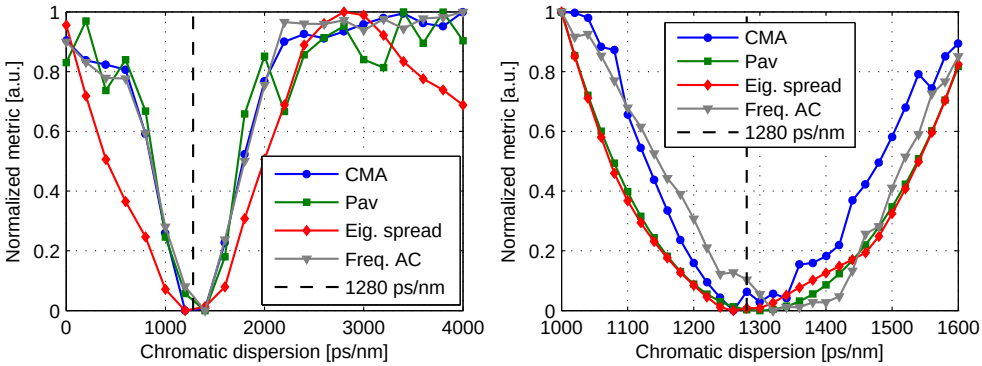

(a) Coarse scan (200 ps/nm) (b) Fine scan (20 ps/nm)

Fig. 2. Comparison of all metrics after normalization to $[0,1]$ range. *Pav* metric was subtracted from 1 for clearness of comparison. Bold dashed vertical line shows the actual value of CD present in the channel (1280 ps/nm).

2.2.1. CMA metric

The first evaluated metric is described in [3, 7] and references provide its evaluation in computer simulations. The algorithm for this metric is based on a modified constant modulus algorithm (CMA) where a deviation from a constant power R_2 is the error function (metric). Since the received signal is sampled at twice the symbol rate, another normalization constant R_1 has to be used. Both R_1 and R_2 have to be constantly estimated from the power of odd and even samples of the received signal. The metric J is then computed

$$J\left[CD\right] = \frac{1}{N}\sum_{k=0}^{N-1}\left(\left|\left|q\left[2k+1\right]\right|^2 - R_1\right| + \left|\left|q\left[2k\right]\right|^2 - R_2\right|\right). \tag{2}$$

The required normalization constants R_1 and R_2 are determined for each block. First, the mean power of odd and even samples, $\bar{q}_1$ and $\bar{q}_2$, is calculated

$$\bar{q}_1 = \frac{1}{N}\sum_{k=0}^{N-1}\left(q\left[2k+1\right]\right)^2 \qquad \bar{q}_2 = \frac{1}{N}\sum_{k=0}^{N-1}\left(q\left[2k\right]\right)^2. \tag{3}$$

Based on the ratio of $\bar{q}_2$ to $\bar{q}_1$, R_1 and R_2 normalization constants are determined as follows:

$$\begin{bmatrix} R_1 & R_2 \end{bmatrix} = \begin{cases} \begin{bmatrix} R_a & R_c \end{bmatrix} & \text{if } \frac{\bar{q}_2}{\bar{q}_1} > \xi \\ \begin{bmatrix} R_b & R_b \end{bmatrix} & \text{if } \xi^{-1} \le \frac{\bar{q}_2}{\bar{q}_1} \le \xi \\ \begin{bmatrix} R_c & R_a \end{bmatrix} & \text{if } \frac{\bar{q}_2}{\bar{q}_1} < \xi^{-1} \end{cases} \tag{4}$$

with proposed empirically adjusted parameters $\xi = 1.25$, $R_a = 0.6$, $R_b = 1.5$ and $R_c = 2$ for the received complex signal power normalized to 1.

The curve of the metric presented in Fig. 2 was averaged over 8 different realizations, each having $N = 256$ samples.

#155788 - $15.00 USD Received 3 Oct 2011; revised 25 Nov 2011; accepted 26 Nov 2011; published 6 Dec 2011

2.2.2. Mean signal power

The second implemented metric is a simplified variant of the CMA-based metric. The mean power of samples at the input to the equalizer

$$P = \frac{1}{N}\sum_{k=0}^{N-1} |p[k]|^2 \tag{5}$$

is compared with the mean power of the signal after CD equalization and decimation to 1 sample/symbol stage. The post-decimation mean power, expressed in terms of signal q at the output of the CD equalizer is given by

$$\widehat{P} = \frac{2}{N}\sum_{k=0}^{\frac{N}{2}-1} |q[2k]|^2 . \tag{6}$$

Next, J metric is found according to

$$J[CD] = \left| P - \widehat{P} \right|, \tag{7}$$

and the estimated value of CD parameter is indicated by the maximum of the metric.

In Fig. 2 the estimated CD value is found at a minimum as the metric was mirrored along the horizontal line at 0.5. Block size chosen for this metric was $N = 2048$.

2.2.3. Eigenvalue spread

An alternative metric, operating with time domain samples, relies on inspection of eigenvalue spread of the autocorrelation matrix. The concept, reviewed in [8], has not been used previously in relation to CD monitoring.

This metric uses samples from the CD equalizer after performing decimation to 1 sample/symbol.

The eigenvalue spread χ of the autocorrelation matrix $\mathbf{R}$ is a quantitative measure of signal distortion. Specifically, $\mathbf{R}$ is the following Toeplitz matrix of size $L \times L$

$$\mathbf{R} = \begin{bmatrix} r(0) & r^*(1) & \cdots & r^*(L-1) \\ r(1) & r(0) & \cdots & r^*(L-2) \\ \vdots & \vdots & \ddots & \vdots \\ r(L-1) & r(L-2) & \cdots & r(0) \end{bmatrix} \tag{8}$$

where r is the autocorrelation of the signal q calculated as

$$r(m) = \sum_{k=L}^{\frac{N}{2}-1} q[2k]\, q^*[2(k-m)] \tag{9}$$

and * denotes complex conjugate. The eigenvalue spread of the autocorrelation matrix and the CD metric itself is then defined as

$$J[CD] = \chi(\mathbf{R}) = \frac{\lambda_{\max}}{\lambda_{\min}}, \tag{10}$$

where $\lambda_{\max}$ and $\lambda_{\min}$ are eigenvalues of $\mathbf{R}$ with the largest and the smallest magnitudes respectively. If the dispersion was correctly compensated, the autocorrelation matrix is well-conditioned and the spread of eigenvalues approaches the theoretical minimum at 1. Otherwise, the matrix is ill-conditioned and the spread is significantly larger than that. This approach allows for construction of a minimum-search metric.

#155788 - $15.00 USD Received 3 Oct 2011; revised 25 Nov 2011; accepted 26 Nov 2011; published 6 Dec 2011

An engineering rule for the autocorrelation matrix size producing good results was found to be

$$L = \frac{CD_{\max} - CD_{\min}}{75}, \tag{11}$$

where in the numerator the maximum and minimum values of CD parameter (expressed in ps/nm) in the range of interest are used (units neglected). It should be noted that eigenvalues computation is an expensive task in terms of required processing power and, therefore, practical use of this metric might be limited.

In the curve shown in Fig. 2, block size was chosen to be $N = 16384$ and matrix size $L = 53$.

2.2.4. Frequency spectrum autocorrelation

The last metric, frequency spectrum autocorrelation, uses post-equalization samples before the inverse fast Fourier transform (IFFT) block. This method was studied in simulation in [4]. It uses signal Q, which is the frequency domain representation of the CD equalizer output after multiplication with the filtering function H_{CD} as presented in Fig. 1. First, a discrete circular autocorrelation is computed

$$U[m] = \frac{1}{N}\sum_{k=0}^{N-1} \mathrm{csgn}\left(\bigcirc_m (Q[k])\right) \cdot Q^*[k], \tag{12}$$

where $\bigcirc_m (Q)$ is a circular shift operator that circularly shifts vector Q by m positions ($m \in N$) and csgn is a complex extension of the sign function sgn, defined as $\mathrm{csgn}(x) = \mathrm{sgn}[\Re(x)] + \imath\,\mathrm{sgn}[\Im(x)]$, with $\Re$ and $\Im$ denoting, respectively, real and imaginary part of a complex number. It is not necessary for m to cover all possible shifts and thus m ranging from $-\lfloor 0.7\frac{N}{2} \rfloor$ up to $\lfloor 0.7\frac{N}{2} \rfloor$ has been used.

The metric function $J[CD]$ for a single CD value under test is then calculated as

$$J[CD] = \sum_m |U[m]|^2, \tag{13}$$

where summation over m covers all applied circular shifts.

The metric curve shown in Fig. 2 was obtained after averaging 20 realizations, each calculated from a block Q of size $N = 256$ samples as to smoothen the obtained curve.

3. Experimental setup

In order to experimentally prove that CD monitoring with the investigated approach is feasible, we use a single branch of a PDM-QPSK transmitter, as outlined in Fig. 3. A pattern generator provides the in-phase and quadrature inputs to the optical modulator at a bit rate of 20 Gbit/s resulting in a 40 Gbit/s QPSK optical signal. In order to test the monitoring algorithms for different magnitudes of CD affecting the signal, two cases are investigated: the back-to-back case (CD negligibly small) and transmission over 80 km of standard single-mode fiber (SSMF) with a dispersion coefficient of approximately 16 ps/nm/km, yielding 1280 ps/nm accumulated CD in total. Back-to-back trial was performed to test if the monitoring algorithm works correctly in a CD-free channel. As the next step, optical noise is added to the signal, varying the optical signal-to-noise ratio (OSNR) from 24 dB, down to 12 dB. An EDFA preamplifier and an attenuator just before the receiver is used to keep the power entering a 100G coherent receiver at a constant level equal to -10 dBm. The local oscillator (LO) is tuned to 1548.88 nm and the signal wavelength is less than 100 MHz apart. The signal and LO lasers are distributed feedback (DFB) narrow linewidth lasers (NLLs). Digital storage oscilloscope (DSO) is used to capture the voltage signal after conversion from optical to electrical domain. Traces are stored and processed offline.

#155788 - $15.00 USD Received 3 Oct 2011; revised 25 Nov 2011; accepted 26 Nov 2011; published 6 Dec 2011

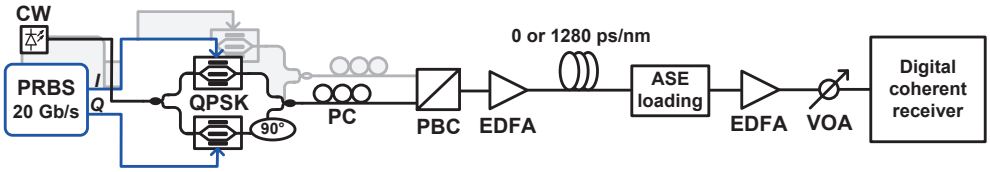

Fig. 3. Experimental setup of the transmission system. CW: continuous wave laser, PRBS: pseudorandom binary sequence generator, PC: polarization controller, PBC: polarization beam combiner, EDFA: erbium-doped fiber amplifier, ASE loading: amplified spontaneous emission noise loading, VOA: variable optical attenuator.

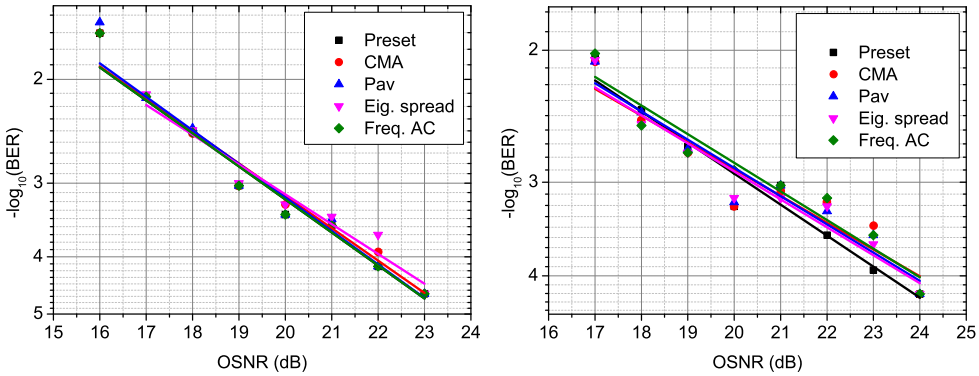

(a) Back-to-back (b) 80 km SMF

Fig. 4. BER vs. OSNR curves for each metric under investigation. *Preset*: reference line based on a priori known CD filter, *CMA*: constant modulus algorithm, *Pav*: mean signal power, *Eig. spread*: eigenvalue spread, *Freq. AC*: frequency spectrum autocorrelation.

4. Experimental results

Figure 4 shows bit error rate (BER) curves after demodulation of the traces using an equalizer driven by the monitoring module, where *Preset* is a reference line showing performance of the receiver when CD filter is manually set with an a priori known CD value of either 0 ps/nm (Fig. 4a) or 1280 ps/nm (Fig. 4b). Remaining lines show the performance of the receiver for different CD metrics as OSNR is varied for both transmission distances. It may be observed that regardless of the CD distortion present in the channel, lines depart only to a very small extent from the reference *Preset* line. This shows that both: each metric and the CD DSP monitor itself are reliable enough as not to introduce any penalty when compared to a CD filter with a fixed CD value. The FIR filter used for polarization demultiplexing is too short to compensate CD after 80 km of fiber transmission; effectively only residual CD is mitigated via the FIR filter, while bulk of the dispersion is removed by the FDE CD equalizer driven by the monitoring module. It is necessary to point out that this proof-of-concept works satisfactory with single polarization QPSK signal and it should be scalable to PDM-QPSK as CD affects both polarizations equally.

5. Conclusions

We experimentally demonstrated the use of DSP OPM algorithms for CD compensation and estimation module preceding timing recovery stage. This allows for an autonomous opera-

#155788 - $15.00 USD Received 3 Oct 2011; revised 25 Nov 2011; accepted 26 Nov 2011; published 6 Dec 2011

tion of a digital coherent receiver in a dispersion non-compensated coherent transport network. To the best of our knowledge this is the first demonstration showing feasibility of the presented receiver arrangement and algorithms in experimental setting. We found out that the four different metrics for assessing dispersion mitigation provide reliable estimations of CD so as no penalty is observed when compared to a CD filter whose value was fixed prior to the transmission.

Acknowledgments

We thank Teraxion for providing PureSpectrum™-NLLs for this experiment. The research leading to these results is partially supported by the CHRON project (Cognitive Heterogeneous Reconfigurable Optical Network) with funding from the European Community's Seventh Framework Programme [FP7/2007-2013] under grant agreement no. 258644.

#155788 - $15.00 USD Received 3 Oct 2011; revised 25 Nov 2011; accepted 26 Nov 2011; published 6 Dec 2011